

The background is a solid purple color with several abstract geometric elements. A large, semi-transparent circular graphic is centered on the right side, featuring concentric rings and a dotted border. Diagonal lines and a grid of small dots are also visible in the lower-left quadrant.

III-5

Life, Earth and
Planetary Sciences

BL4U

Quantitative Penetration Profiles of Free and Nanocarrier-Bound Dexamethasone in Human Skin Studied by Soft X-Ray Spectromicroscopy

K. Yamamoto¹, T. Ohigashi², Y. F. Wang², S. Hedtrich³, F. Rancan⁴, R. Flesch¹, A. Klossek¹, E. Fleige¹, S. Ahlberg⁴, A. Vogt⁴, U. Blume-Peytavi⁴, P. Schrade⁵, S. Bachmann⁵, R. Haag¹, M. Schäfer-Korting³, N. Kosugi² and E. Rühl¹

¹Institute for Chemistry and Biochemistry, Freie Universität Berlin, Takustr. 3, 14195 Berlin, Germany

²UVSOR Facility, Institute for Molecular Science, Okazaki 444-8585, Japan

³Institut für Pharmazie, Freie Universität Berlin, 14195 Berlin, Germany

⁴Charité Universitätsmedizin, 10117 Berlin, Germany

⁵Abteilung für Elektronenmikroskopie at CVK, 13353 Berlin, Germany

The penetration of topically applied drugs in skin is known to be enhanced by drug nanocarriers [1]. However, quantitative drug uptake studies with high spatial resolution in which the exposure time and drug formulation are systematically varied are lacking to date. We have investigated the uptake of the anti-inflammatory drug dexamethasone by human skin using soft X-ray spectromicroscopy.

Chemical selectivity of this approach is gained by excitation of the O 1s→ π^* -transition of dexamethasone at 530.65 eV, which is suitable to suppress the background absorption of fixed human skin as well as drug nanocarriers (core-multi-shell nanocarriers (CMS)), which were loaded by 5% dexamethasone. In addition, we used two different exposure times (4 h and 16 h) and varied the drug formulation, where either ethanolic solution or HEC gel (drug concentration: 0.5%) were used, respectively. Any cross sensitivities from absorption of untreated skin were subtracted, so that exclusively the drug concentration was monitored.

The experiments were performed at the BL4U beamline at UVSOR III using a scanning X-ray microscope (STXM), similar to previous work, in which the feasibility of this approach was explored [2,3].

Figure 1 shows a comparison of depth profiles of dexamethasone in different skin samples along with an optical micrograph, in which the skin regions are labeled (stratum corneum (SC), viable epidermis (VE), and dermis (D)). Figure 2 shows the integrated drug concentration for the samples under study, which facilitates to derive quantitative information regarding the drug distribution, if the exposure time and drug formulation are varied. Specifically, Fig. 1(a) indicates that after 4 h most of the drug is found in the SC, whereas a lower fraction is found in the VE (cf. Fig. 2). No drug is observed in the dermis (D). This situation changes, when 16 h of drug exposure in HEC gel are used (cf. Fig. 1(b) and Fig. 2). The intense maximum in the SC is weaker and the drug concentration in the VE is enhanced. If drug nanocarriers in HEC gel are used instead of the neat drug (cf. Fig. 1(c)), no drug signal was observed after 16 h in the SC rather than in the VE. This underscores the expected drug transport into deeper skin layers by

nanocarriers. A drop in local drug concentration is observed for all samples in the dermis (D). This indicates that in this region rapid clearance is possible, so that no enhanced drug concentration is observed.

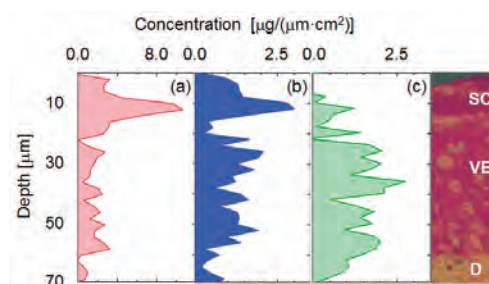


Fig. 1. Distribution of dexamethasone in the top skin layers (right hand side: typical optical micrograph, see text for details): (a) dexamethasone in ethanol: exposure time: 4 h; (b) dexamethasone in HEC gel: exposure time: 16 h; (c) CMS nanocarriers in HEC gel, exposure time: 16 h.

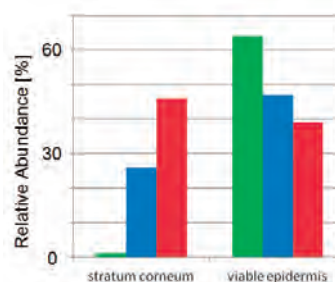


Fig. 2. Relative abundance of dexamethasone in the stratum corneum and viable epidermis (green: drug-loaded CMS nanocarriers in HEC gel, exposure time: 16 h; blue: dexamethasone in HEC gel: exposure time: 16 h; red: dexamethasone in ethanol: exposure time: 4 h) compared to the dose applied to skin.

[1] N. Alnasif, C. Zoschke, E. Fleige, R. Brodewolf, A. Boreham, E. Rühl, K.-M. Eckl, H.-F. Merk, H.-C. Hennies, U. Alexiev, R. Haag, S. Kuchler and M. Schäfer-Korting, *J. Control. Rel.* **185** (2014) 45.

[2] R. Flesch *et al.*, *UVSOR Activity Report 2013* **41** (2014) 156.

[3] K. Yamamoto, *et al.*, *Anal. Chem.*, *accepted* (2015) DOI : 10.1021/acs.analchem.5b00800

BL4U

Evaluation of Sample Damage of XANES and Application to the Analysis of Carbonaceous Materials in Hayabusa-Returned Samples

M. Uesugi and A. Nakato

Institute of Space and Astronautical Science, Japan aerospace exploration agency, Sagami-hara 252-5210, Japan

Hayabusa spacecraft has successfully retrieved regolith particles from the surface of asteroid Itokawa. Silicate materials found in the sample catcher of the Hayabusa spacecraft were typically 50 μ m in diameter, and their origin was confirmed by mineralogical, chemical and isotopic analyses in the preliminary examination of the Hayabusa- returned particles [e.g. 1-6].

Carbonaceous particles, those have been found in the sample catcher together with silicate particles, were still under the investigations, including precise determination of their origin. Results of isotopic analysis of H, C and N of the carbonaceous materials by NanoSIMS did not show any signatures of their extraterrestrial origin, i.e. isotopic anomalies against the terrestrial composition [7]. Some of the results of analyses by Transmission Electron Microscopy (TEM, [8]) and X-ray absorption near edge structure (XANES, [9]) indicated relation to the terrestrial material. Thus, those particles might indicate the contamination of terrestrial material into the sample catcher before, during and/or after the operation of Hayabusa spacecraft.

XANES analysis of C, N and O is useful for the characterization of molecular structure of the unknown carbonaceous material, which would relate to their origin. We expected to obtain the information for the source of contamination of Hayabusa spacecraft by comparing possible contaminants and Hayabusa-returned samples using XANES/STXM installed in UVSOR.

It is well known that high voltage electron beam of TEM could modify the C-XANES spectrum largely [9]. Thus TEM observation has generally been applied after XANES analysis. However, in this study, we focused on the sample damage induced C-XANES. To evaluate the damage, TEM observations were done before and after C-XANES analysis. As the results, TEM observations (Fig. 1) clearly show that if the sample contains NaCl or KCl inclusions, they would be damaged heavily by the XANES analysis. The phenomenon was also observed in the samples analyzed by other XANES/STXM instrument, though the detail of the process is uncertain.

This result should be important not only for the analyses of Hayabusa-returned samples, but also for the future analyses of Hayabusa2 returned samples. Because the amount of sample obtained directly by spacecraft is very small, sequential analysis will be inevitable for the characterization of those samples. In this case, we should construct the analytical flow

based on the sample damage effective to the downstream analyses. Results of XANES analyses of a Hayabusa-returned sample, RA-QD02-0180-03, showed clear relation to the particles collected by witness plates those exposed to the cleanroom of Hayabusa2 spacecraft, though the data should be re-examined carefully (in progress).

In future work, we will apply the XANES/STXM analysis to further possible contaminants such as rubbers and particles of biological materials, for the precise determination of the origin of carbonaceous particles in Hayabusa-returned samples.

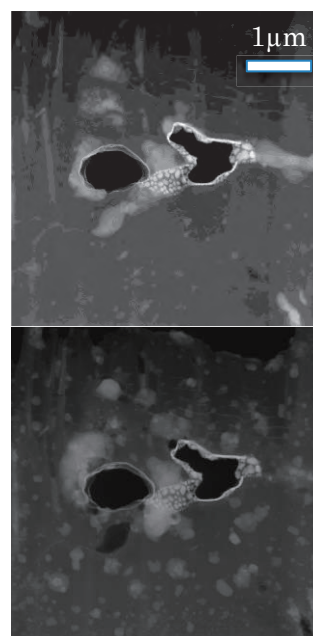


Fig. 1. STEM/DF image of the Ultra-thin section of carbonaceous material of a Hayabusa-returned sample, RA-QD02-0180-03 before (upper) and after (lower) the C-XANES analysis. White objects are the NaCl and KCl inclusions. We can observe the disrupted inclusions entire section after the C-XANES analysis.

- [1] T. Nakamura *et al.*, *Science* **333** (2011) 1113.
- [2] H. Yurimoto *et al.*, *Science* **333** (2011) 1116.
- [3] M. Ebihara *et al.*, *Science* **333** (2011) 1119.
- [4] A. Tsuchiyama *et al.*, *Science* **333** (2011) 1121.
- [5] T. Noguchi *et al.*, *Science* **333** (2011) 1125.
- [6] K. Nagao *et al.*, *Science* **333** (2011) 1128.
- [7] M. Ito *et al.*, *Earth planet. Space* **66** (2014) 102.
- [8] M. Uesugi *et al.*, *Earth planet. Space* **66** (2014) 102.
- [9] H. Yabuta *et al.*, *Earth planet. Space* **66** (2014) 156.

BL4U

Absorption Spectra of Bio-Cell Organelles in Cultural Fluid

T. Ejima¹, M. Kado², M. Aoyama³, K. Yasuda³ and T. Tamotsu³

¹IMRAM, Tohoku University, Sendai 980-8577, Japan

²Japan Atomic Energy Agency, Kizugawa 619-0215, Japan

³Dept. of Biological Sciences, Fac. of Science, Nara Women's University, Nara 630-8263, Japan

Organelles in bio-cells are composed of proteins, and the proteins consist of specific 20 kinds of amino acids. Spectra of these amino acids are known at C-K and N-K absorption edges [1], therefore absorption spectrum of a small organelle will be interpreted by a spectral combination of these amino acids in zero-th order approximation. If both position of organelles in a bio-cell and C-K and/or N-K absorption spectra at the organelles are measured simultaneously, positions and compositions of the organelles will be obtained in the bio-cell. Water-window wavelength region ($\lambda=2.3-4.5\text{nm}$) is suitable for this simultaneous measurements, because water is transparent and carbides and nitrides are absorbable, which are the principal components of proteins. On the other hand, the measurements have hardly been made especially for bio-cells of eukaryotes, because thickness of the eukaryotes cells is thick for absorption spectroscopy even in Water-window wavelength region. In addition, usual analytical method takes much time to separate the positions and spectra from measured SX images.

In this study, a Leydig cell in a mouse testis was used and thickness of the bio-cell was controlled with culture fluid under $5\ \mu\text{m}$ thick by a sample holder. The thickness of the Leydig cell contained in the sample holder was measured by an interference

method, therefore the thickness of the bio-cells were confirmed as $5\ \mu\text{m}$ or less. The SX images of the Leydig cells were taken under the spatial resolution of 200nm at around N-K absorption edge. Spectra and positions of the organelles in the Leydig cell were separated from the measured SX images by the use of image analysis methods [2], and absorption coefficients of the separated structures are also obtained. Obtained spectra are composed mainly of σ^* and π^* bonds, and shapes of small structures in the bio-cell depend on the density of the organelles.

[1] for example, Y. Zubavichus, A. Shaporenko, V. Korolkov, M. Grunze and M. Zharnikov, *J. Phys. Chem. B* **112** (2008) 13711.

[2] M. Lerotic, C. Jacobsen, J. B. Gillow, A. J. Francis, S. Wirick, S. Vogt and J. Maser, *J. Elec. Spectro. Rel. Phenom.* **144-147** (2005) 1137.

Acknowledgements

This work was supported by JSPS KAKENHI Grant Numbers 23241038 and by Nanotechnology Platform Program (S-13-MS-1002) of MEXT, Japan.

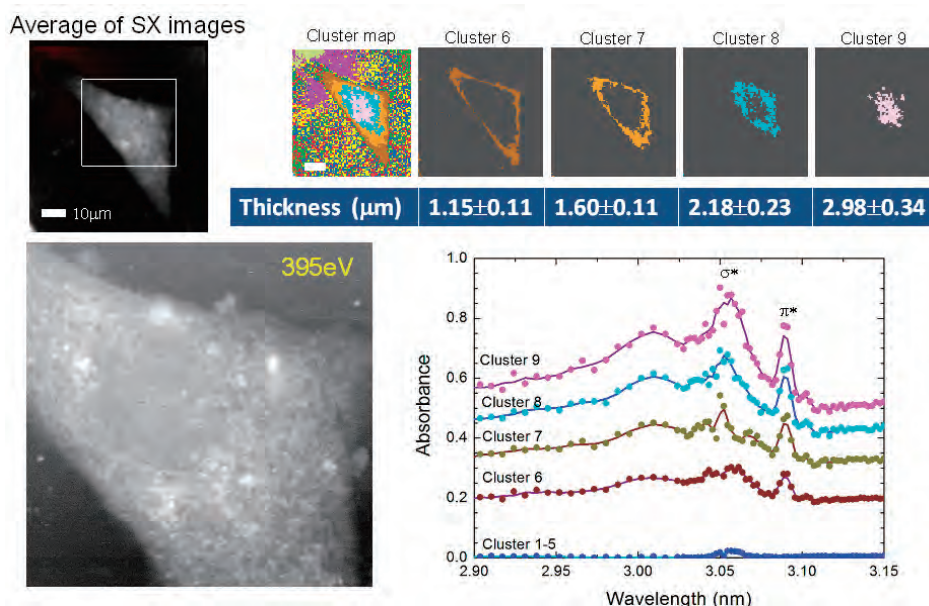


Fig. 1. From the measured sx images, cluster structures were separated according to the similar spectrum of each dot in the images. It are presented in the figure that an average sx image of the measured sx images (upper left), details of sx image at 395 eV (lower left), clusters separated and its thicknesses measured by an interference method (upper right), and absorption spectra of the clusters obtained from sx images (lower right).

BL4U

Evaluation of FIB Beam Damage in XANES Spectra of Organics in Meteorites: Preliminary Measurements for Implementation Planning of a Synchrotron Cosmochemistry Research Base at UVSOR BL4U

H. Yabuta¹, A. Takahashi¹, Y. Inagaki² and T. Ohigashi²

¹Department of Earth and Space Science, Osaka University, Osaka 560-0043, Japan

²UVSOR Facility, Institute for Molecular Science, Okazaki, 444-8585, Japan

This study aimed to evaluation of FIB beam damage in XANES spectra of organics in meteorites. However, unfortunately, it was impossible to carry out the analysis during the beam time in June, 2014, due to a mistake by a manufacturer (a maker) of placing a diffraction grating upside down, after their cleaning the carbon contamination. For this reason, the schedule had to be changed, and the analogue of organic materials in meteorite was analyzed by STXM during the beam time in December 2014. Carbon contamination on the surface of the mirror was still remained and it was difficult to acquire an ideal Carbon-XANES spectrum, and the measurements were limited to Nitrogen-XANES.

Paraformaldehyde (120 mg), glycolaldehyde (120 mg), $\text{NH}_3(\text{aq})$ (54 μl), $\text{Ca}(\text{OH})_2$ (30 mg) in 2 ml of water in a glass tube was heated at 90°C for 3-100 days [1-2]. After heating, the precipitation was rinsed with HCl and dried. The purified organic solids were suspended in ethanol and the suspension was dripped to the Cu-TEM grid (200 mesh) with SiO film using a micropipette. N-XANES spectra of the samples were acquired using a scanning transmission x-ray microscope (STXM) at the BL 4U, UVSOR.

Our previous study revealed that the organic solids include a number of micro spherules of 3-20 μm in diameter. Their size and shape distributions changed with a heating period of time. In contrast, N-XANES spectra of the organic solids were similar throughout a heating period of time (Fig. 1), exhibiting absorption peaks of imine ($\text{C}=\text{N}$) at 398.8 eV, protonated imine ($\text{C}=\text{NH}^+$) at 400.8 eV, and amide ($\text{NHx}(\text{C}=\text{O})\text{C}$) around at 401.6 eV, respectively. Combining the results by infrared analysis, these features imply that the organic microspherule is a self-organized polymer of a amphiphilic molecule including alkyl group and pi-bonding.

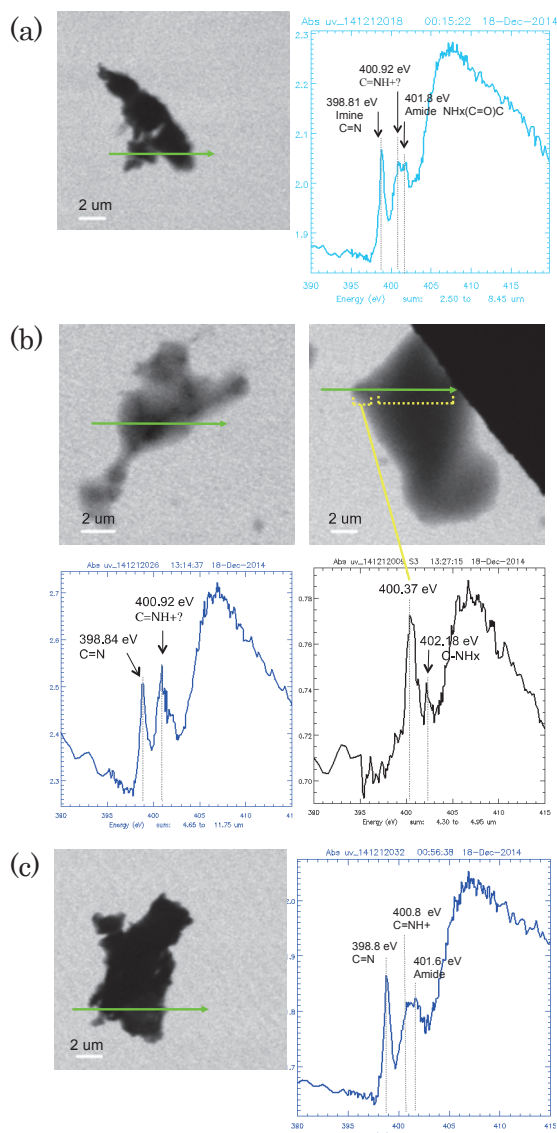


Fig. 1. N-XANES spectra of analogues of organic materials in meteorite, which were synthesized from formaldehyde and ammonia for different heating periods of times (a) 10 days, (b) 20 days, and (c) 60 days.

[1] G. D. Cody, E. Heying, C. M. O.'D. Alexander, L. R. Nittler, A. L. D. Kilcoyne, S. A. Sandford and R. M. Stroud, *PNAS* **108** (2011) 19171.

[2] Y. Kebukawa, A. L. D. Kilcoyne and G. D. Cody, *Astrophys. J.* **771** (2013) 19.

BL4U

Chemical Mapping of DNA and Protein in Isolated Cell Nuclei during Apoptotic Process Using STXM

A. Ito^{1,2}, T. Ohigashi^{2,3}, K. Shinohara¹, S. Tone⁴, M. Kado⁵, Y. Inagaki² and N. Kosugi²

¹*School of Engineering, Tokai University, Hiratsuka 259-1292, Japan*

²*UVSOR Facility, Institute for Molecular Science, Okazaki 444-8585, Japan*

³*The Graduate University for Advanced Studies (SOKENDAI), Okazaki 444-8585, Japan*

⁴*Department of Biochemistry, Kawasaki Medical School, Kurashiki 701-0192, Japan*

⁵*Japan Atomic Energy Agency, Kizugawa 619-0215, Japan*

Apoptosis is characterized as a programmed cell death controlled by the expression of the relating genes. One of the remarkable morphological features of cells which undergo apoptosis is the deformation of nuclei during the apoptotic process. Tone et al. observed the distribution change of DNA in isolated cell nuclei with the progression of apoptosis by labelling DNA with fluorescent dye [1]. They classified the apoptotic process into three characteristic stages, stage 1, 2 and 3. DNA in the normal nuclei (stage 0) proceeds to ring-shape structure (stage 1) accumulated in the peripheral region, followed by necklace-shape structure where the ring structure is broken intermittently (stage 2). Finally the nuclei are collapsed toward the center (stage 3). In the present study, we observed distributions of DNA as well as nuclear protein including histone, using chemical mapping of STXM with higher spatial resolution than optical microscope. Our previous study for the DNA mapping in mammalian cell nuclei was successfully achieved with the aid of the different XANES profiles between DNA and protein at the N-K absorption edge [2]. Chemical mapping was extended to apoptotic nuclei in this study.

XANES profiles of DNA and histone were measured by the STXM around the N-K absorption edge from 390 to 410 eV as reference spectra. Solution of these biomolecules was dropped on collodion membrane supported by an EM grid, and then dried in the air. S/M extract of chicken DU249 cells was used to induce apoptosis on isolated nuclei of human HeLa S3 cells. The nuclei were fixed with glutaraldehyde at the timing of four different stages described above, and dropped on Formvar membrane supported by EM grid, and then dried in the air.

The 61 X-ray transmission images (an energy stack) for each stage were acquired from 397 to 403 eV. The dwell time and scanning pitch were 10 ms and 0.1 μm , respectively. DNA and histone (protein) distributions were obtained fitting the reference spectra of DNA and histone to the energy stack by using aXis2000 software (fitting method). Alternatively the maps were obtained by the subtraction of images taken between at the top and the bottom of the resonance peak of DNA or histone (subtraction method).

Figure 1 shows distributions of DNA and protein in

four stages of apoptosis. In the case of normal nuclei at the stage 0 shown by the panel a, b and c, DNA and protein were distributed in the nearly whole nucleus with similar pattern, since nucleus mainly consists of chromatin, a complex structure of DNA and proteins. At the stage 1, DNA and protein were accumulated in the ring shape on the rim of nucleus (panel e and f). The width of the ring was less than 0.5 μm . Note that in the central part of the nucleus DNA seems to be distributed more preferentially than protein. In addition, an image of “constant” (panel g), which means the existence of molecules with no spectral feature at the N-K absorption edge, shows significant distribution in the inner region. The identification of the molecules is an issue for the future research. These distributions of DNA and protein were also confirmed by the subtraction method. For the stages 2 and 3, remarkable difference was not observed between DNA and protein maps. Necklace structure in the stage 2 as shown by arrows in panel h was evident in both DNA and protein maps. To improve the quality of the images, reproducibility of reference spectra and the acquisition time to assure enough photon counts per pixel should be considered.

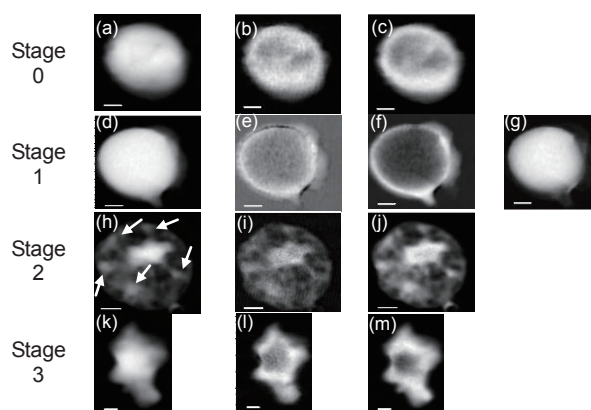


Fig. 1 Distributions of DNA and protein in four stages of apoptotic nuclei.

X-ray image at 397 eV: (a), (d), (h), (k); DNA map: (b), (e), (i), (l); protein map: (c), (f), (j), (m); constant map: (g)

bar: 1 μm (stage 0, 1, 3), 2 μm (stage 2)

[1] Toné *et al.*, *Exp. Cell Res.* **313** (2007) 3635.

[2] T. Ohigashi *et al.*, *UVSOR Activity Report* 2013 **41** (2014) 158.

BL4U

Observation of Prokaryotic Organelles of Musty-Odor Producing Filamentous Cyanobacterium Using STXM

K. Takemoto^{1,2}, M. Yoshimura², T. Ohigashi^{2,3} and H. Kihara^{2,4}

¹Department of Physics, Kansai Medical University, Hirakata 573-1010, Japan

²SR center, Ritsumeikan University, Kusatsu 525-8577, Japan

³UVSOR Facility, Institute for Molecular Science, Okazaki 444-8585, Japan

⁴Himeji Hinomoto College, Himeji 679-2151, Japan

In a source of potable water, musty-odor produced by blue-green algae suddenly appear all over the world. Since 1969, a problem of musty-odor in potable water has occurred due to sudden propagation of *Phormidium tenue* (*Pseudanabaena* sp.) green strain (PTG) in Lake Biwa. Because there are few studies on PTG, an exhaustive study of PTG is required of water resource managers.

PTG is a small filamentous cyanobacterium, and the trichome consists of cells 1.0–1.6 μm in width, and 2.5–10 μm in length. Due to a diffraction limit, light microscope (LM) is impossible to provide intracellular observation with a sufficient spatial resolution. Therefore, we applied a soft X-ray microscope (XM) to PTG observation. The XM is capable of imaging thick and untreated specimens, allowing viewers to investigate whole cells up to 10 μm thick with much higher resolution than LM. In our full field transmission soft XM observation, several intracellular granules were observed. [1].

Based on the transmission electron microscopy (TEM) observation and the energy dispersive X-ray (EDX) analysis on low temperature/low vacuum scanning electron microscope (LT/LV SEM), we inferred that the granules were polyphosphate and/or carboxysome. Carboxysome is one of the bacterial microcompartment that contains enzymes, RuBisCO, involved in carbon dioxide fixation. Polyphosphate granule is one of the bacterial microcompartment that is characterized by their high content of phosphorus. Polyphosphate has the general formula $M_{(n+2)}P_nO_{(3n+1)}$, where M is H^+ or monovalent metal cation [2]. However, there is no objective evidence to identify them. In this study, it is aimed to obtain the objective evidence to identify them using oxygen K-edge X-ray absorption near edge structure (XANES).

Oxygen K-edge XANES spectra were collected on the scanning transmission X-ray microscope (STXM) at UVSOR BL4U [3]. PTG was isolated from Lake Biwa and culture was carried out under the fixed condition for four weeks [1].

Figure 1 shows a STXM image of the distribution of oxygen in PTG. Four oxygen accumulated granules were confirmed. Characterization of intracellular granules was performed by oxygen K-edge XANES (Fig. 2). The spectrum from cytoplasm shows an intense pre-peak. On the other hand, the spectrum from granule shows a small pre-peak at the same

energy region. Although the pre-peak energies are almost similar, the main edge energy of the granule shifts towards lower than that of cytoplasm. To identify the granules, we intend to promote a more detailed analysis.

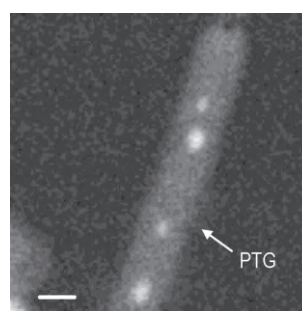


Fig. 1. Distribution of oxygen in PTG. Scale bar is 1 μm .

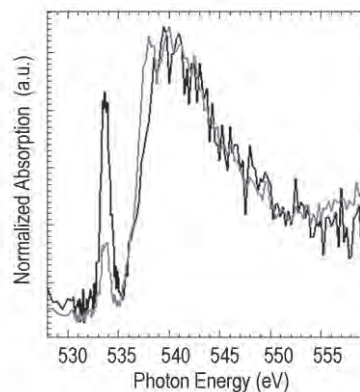


Fig. 2. Oxygen-XANES spectra of cytoplasm (black line) and granule (gray line).

[1] K. Takemoto *et al.*, Jpn. J. Water Treat. Biol. **48** (2012) 157. [in Japanese.]

[2] I.S. Kulaev *et al.*, The Biochemistry of Inorganic Polyphosphates, 2nd Ed., John Wiley & Sons, Inc., New York (2004) 3.

[3] T. Ohigashi *et al.*, J. Phys. Conf. Ser. **463** (2013) 012006.

BL4U

Skin Penetration Study of Drug Carriers Using Soft X-Ray Spectromicroscopy

P. Pan-In¹, T. Ohigashi^{2,3}, N. Kosugi^{2,3} and S. Wanichwecharungruang¹

¹Department of Chemistry, Faculty of Science, Chulalongkorn University, Bangkok 10330, Thailand

²UVSOR Facility, Institute for Molecular Science, Okazaki 444-8585, Japan

³School of Physical Sciences, The Graduate University for Advanced Studies (SOKENDAI), Okazaki 444-8585, Japan

Skin is a natural barrier to protect human body and control molecular transports from and into the body. Nanoparticles can be developed to deliver drugs both into the skin and through the skin into the circulation. Although it has been stated that drug/bioactive molecules can penetrate through skin barrier via intracellular, intercellular and follicular pathways [1, 2], recent researches have proven that the follicular pathway is important for the nanoparticulate drug delivery systems [3]. Researchers have shown that nanoparticles with appropriated sizes could penetrate well into skin via hair follicle because the rigid hair shafts acted as the geared pump that upon movement or massage the particles could be pushed down. The loaded drugs could then be stored more than 10 days in hair follicles [3].

Thus, the aim of this research is to study the skin penetration level of oxidized carbon nanoparticles with the size between 150-800 nm [4]. BODIPY® FL (4,4-Difluoro-5,7-Dimethyl-4-Bora-3a,4a-Diaza-s-Indacene-3-Propionic Acid) was grafted on the particles. Porcine skin penetration of the particles was investigated *ex vivo*. The BODIPY-grafted particles were massaged on fresh porcine skin samples at the coverage of 100 µg/cm² and the applied skin was left for 30 minutes before being subjected to the treatment with 4% glutaraldehyde and then cryo-sectioning. The thickness of the skin sections was 400 nm. Then, the skin samples were mounted on Cu grids (300-mech) and subjected to the soft X-ray microscopic investigation. The experiment was carried out at the B 1s-edge (170-200 eV) for tracking the BODIPY-grafted particles.

The soft X-ray experiment was performed at the BL4U beamline at UVSOR using a scanning X-ray microscope (STXM) [5]. The experimental design was that the presence of the boron element in the BODIPY® FL (Fig. 1) could make a significant difference in X-ray signal when compared to signals from tissue with no BODIPY® FL. Chemical selectivity was obtained from excitation at the B 1s-edge (170-200 eV). The presence of the 182 eV peak observed in the B 1s-absorption of only the BODIPY-grafted particles, not the skin tissue (Fig. 2), provided a chemical selectivity for tracking the carrier uptake into porcine skin.

Unfortunately, the (BODIPY-grafted particle)-treated porcine skin samples did not show any obvious 182 eV peak in their B 1s spectra, even at the

very uppermost location where the carriers were applied. We speculate a too low concentration of the BODIPY moieties in the particles. To investigate for the skin penetration ability of this carrier in the future, a more intense BODIPY labeling will be required. In addition, skin application at a high dose will be needed.

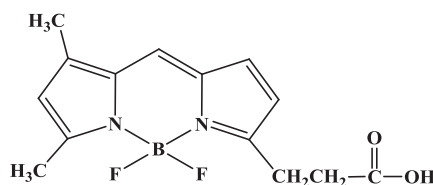


Fig. 1. Structure of BODIPY® FL.

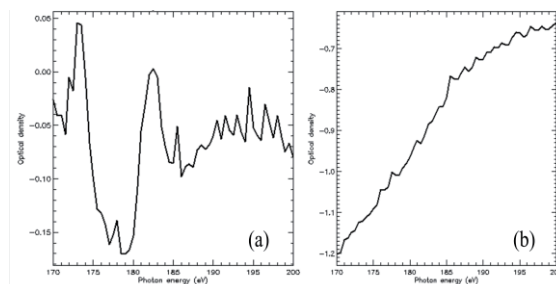


Fig. 2. B 1s excitation of BODIPY-grafted particles (a) and porcine skin (b).

[1] M. A. Bolzinger *et al.*, *Curr. Opin. Colloid Interface Sci.* **17** (2012) 156.

[2] K. Moser *et al.*, *Eur. J. Pharm. Biopharm.* **52** (2001) 103.

[3] J. Lademann *et al.*, *Skin Pharmacol. Physiol.* **19** (2006) 232.

[4] S. Arayachukiat *et al.*, *Nano Lett.* Accepted (2015).

[5] T. Ohigashi *et al.*, *J. Phys.: Conf. Ser.* **463** (2013) 012006.

Farewell Parties

